2.1. Definitions of Velocity, Displacement, Strain and Strain Rate

Cardiac motion and deformation occur in three dimensions. The heart rotates and repositions (circumferential), shortens and dilates in longitudinal direction and thickens and relaxes in radial orientation during cardiac cycle (Figure 10).
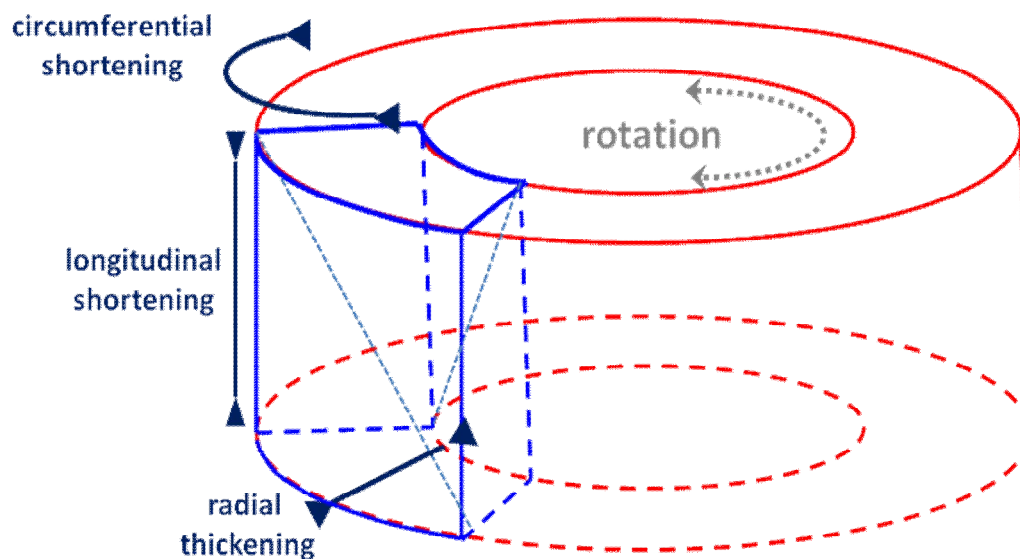

Fig. 10. 3D-illustration of a hypothetical myocardial segment. Myocardial motion and deformation consist of three major components: longitudinal, radial and circumferential. The total deformation of a myocardial segment is very complex and includes shortening, thickening and rotatory movement. Figure reproduced from (69).

In our study we investigate all parameters in one-direction, therefore, motion and deformation is considered as one-dimensional. This dimension was the longitudinal axis of the ventricle.

2.1.1. Definitions related to Motion; Velocity and Displacement

The amount of motion normalized to time is defined to be the velocity of the object. It is thus the displacement of the object divided by the time required to make the displacement. [The object in Tissue Tracking Echocardiography (TTE) is mainly a single point or a Region of Interest (ROI).] Hence, its unit is cm/s. Velocity is used to describe how fast the myocardium moves in a particular direction. During systole myocardium travels towards apex and velocities are positive in nature. During diastole heart muscle moves to its initial position and diastolic velocities are negative. Displacement is the measure defining how far a myocardial segment moves from an initial point. In fetal echocardiography its unit is mm and indicated positively.

2.1.2. Definitions related to Deformation

2.1.2.1. Strain

Strain (S) is defined as the deformation of an object, normalized to its original shape. In a one-dimensional concept the only possible deformation is lengthening or shortening. This is illustrated in Figure 11. By convention, the expression is defined in such a way that lengthening is represented as a positive value for S, while shortening is represented by a negative value (Figure 12). When the length of an object is known before (at the state of L_0) and at the end of deformation (L_1 at a random time frame) Lagrangian strain can be defined. However the deformation of the object can also be expressed relative to the length at a previous time instance (natural strain). According to this approach it is possible to evaluate the amount of deformation occurring during an infinitesimal time interval. For cardiac applications, it has been suggested that it may be more appropriate to measure natural strain, since the values measured are less dependent on the definition of the initial length L_0 rather than on a previous time instance (70). However, most current cardiac imaging techniques (echocardiography, magnetic resonance imaging, radionuclear imaging, angiography) including utilized one in our study measure Lagrangian strain. Since strain is a proportion, it is expressed in percent (%).

Longitudinal Direction

End Diastole   End Systole

Strain (%):

$$\frac{L - L_o}{L_o}$$

L_0 L

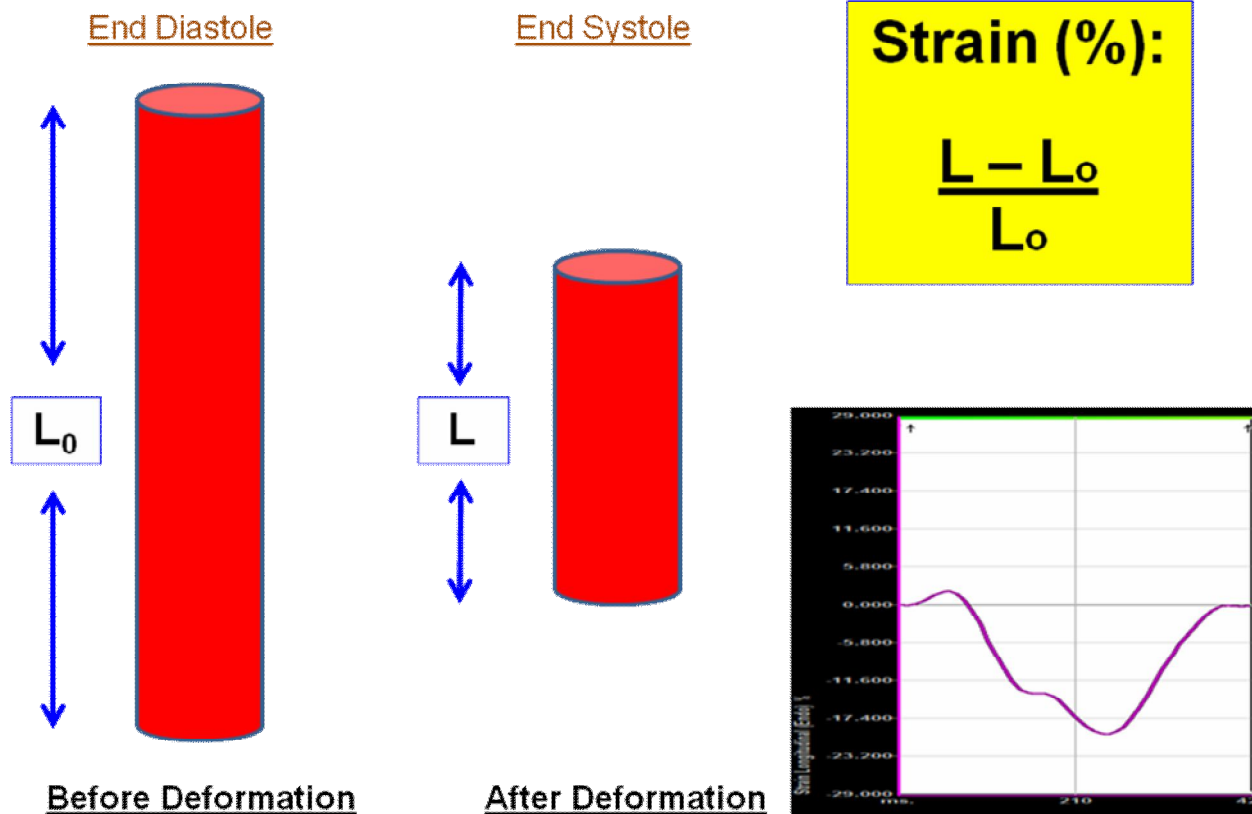Before Deformation   After Deformation

Fig. 11. Strain pattern of a region of the heart in the longitudinal direction. L_0; original length at end diastole, L; length after deformation. At the right lower corner a Strain curve example.

- 20 %
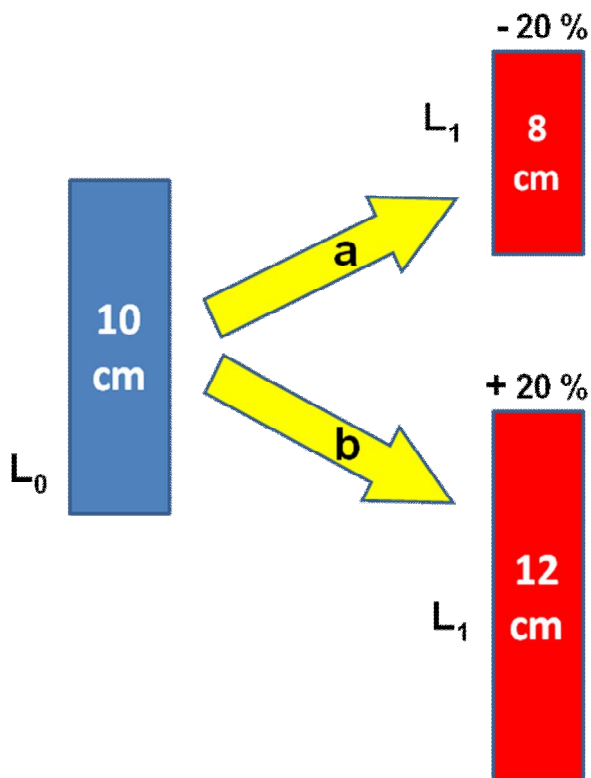
L_1 8 cm

10 cm

a

L_0

+ 20 %

b

L_1 12 cm

Fig. 12. Schema illustrating the negative and positive strain (S). S is the change in length normalized to initial length of muscle (Lo). Thus, decrease in length (a) (such as occurring in muscle contraction) would result in negative S, increase in length (muscle relaxation) (b) would result in positive S. L_0, Initial length of muscle; L_1, final length.

2.1.2.2. Strain Rate (SR)

Strain Rate is the speed at which deformation (i.e. strain) occurs and has the unit s^{-1}. (Figure 13)
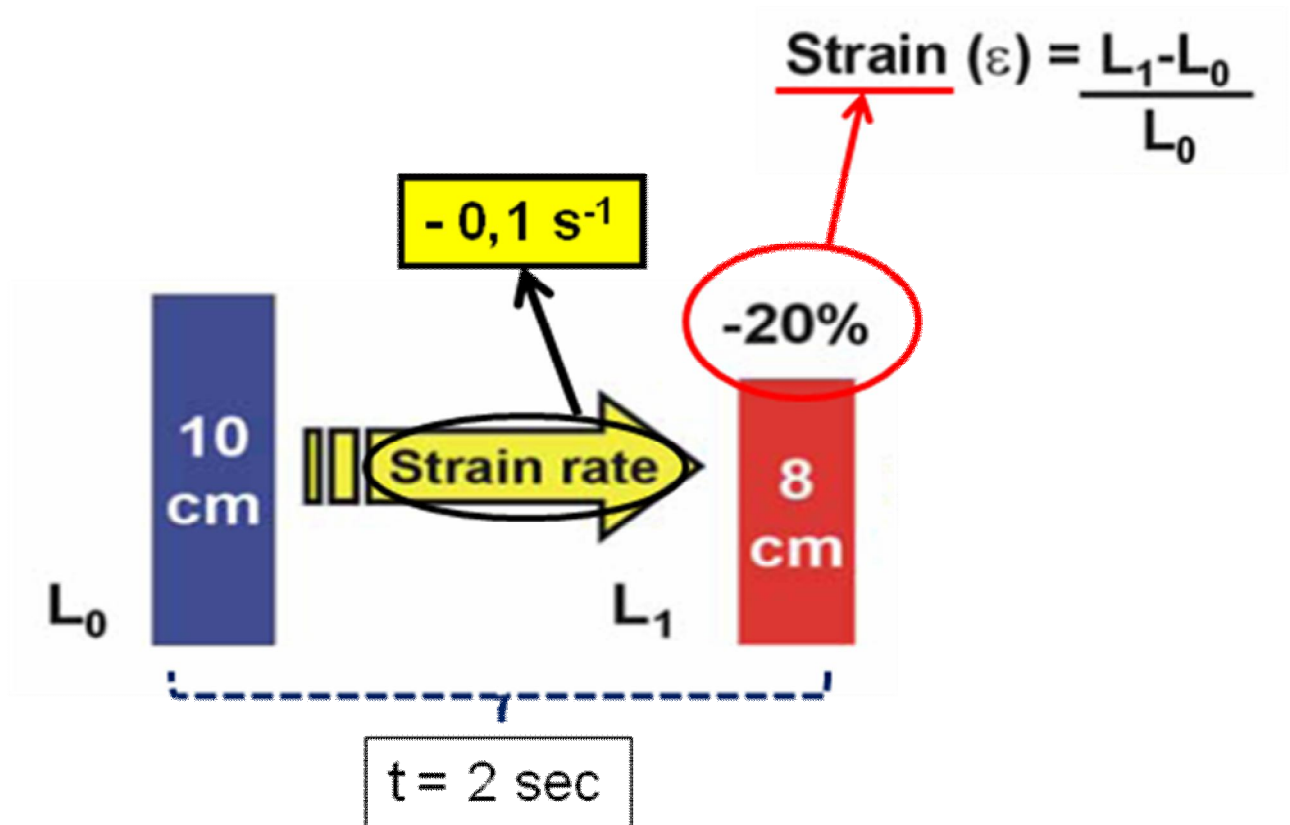

Fig. 13. Figure to illustrate the relationship between S and SR. If we assume that this deformation (in this case the shortening) takes 2 seconds, the strain rate is equal to - 0,2/2 sec, which is - 0,1s^{-1}. Figure reproduced from (71).

2.2. Tissue Tracking Echocardiography (TTE)

2.2.1. Feature Tracking Algorithm

In recent years there has been extensive research to quantify regional and global myocardial function. Feature Tracking is a novel algorithm that investigates overall and segmental LV performance using new parameters such as strain and strain rate. It incorporates ultrasound speckle and endocardial contour tracking with mitral annulus motion, tissue-blood border detection and the periodicity of the cardiac cycle. (18) Commercially available software programs from different medical solution providers utilize various tissue tracking models and allow automatic evaluation of the dynamic properties of the endocardial border and of the sub-endocardial tissue from 2D B-Mode echocardiograhic clips. Their difference is based on the type of algorithm employed; the first (and in adult cardiology more investigated) method is known as "speckle tracking" and the second one is known as "feature tracking". This study uses the latter method which relies on the algorithm of "Optical Flow Analysis".

2.2.1.1. Tracking of the Reference Points – Initial Steps

In this method the endocardial border, drawn by the operator, is identified as a sequence of points. It is then automatically followed frame by frame by searching in the gray-scale pattern for each single point, in the neighbourhood of maximum likelihood (Figure 14). The algorithm performs an adaptive control based on the spatial coherence of points with respect to the points fixed by the operator. This way the recognition of atrioventricular valve level is ensured (Figure 15). The algorithm additionally analyzes displacement of all the points tracked in two spatial dimensions (along the endocardial border and perpendicular to it) as shown on Figure 16 and 17.
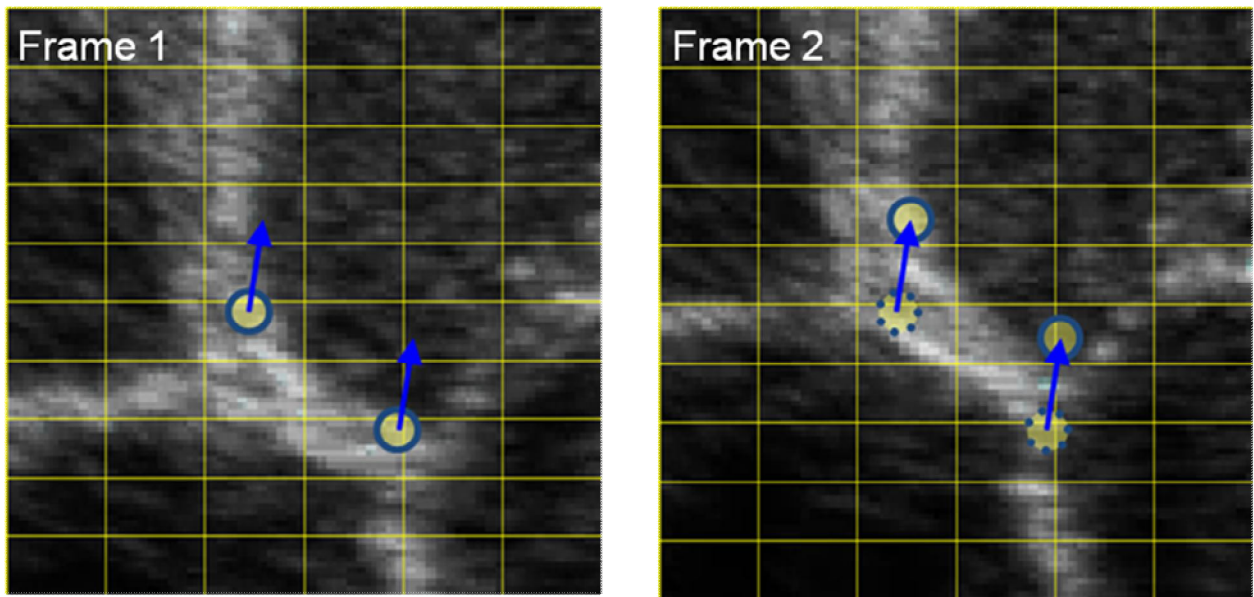
Fig. 14. One of the basic components of any Tissue Tracking (TT) algorithm is the following of the moving grey-scale information from one frame to the next frame. This ensures to evaluate the displacement at every recognizable point. Figure adapted from Pedrizzetti et al. (72)
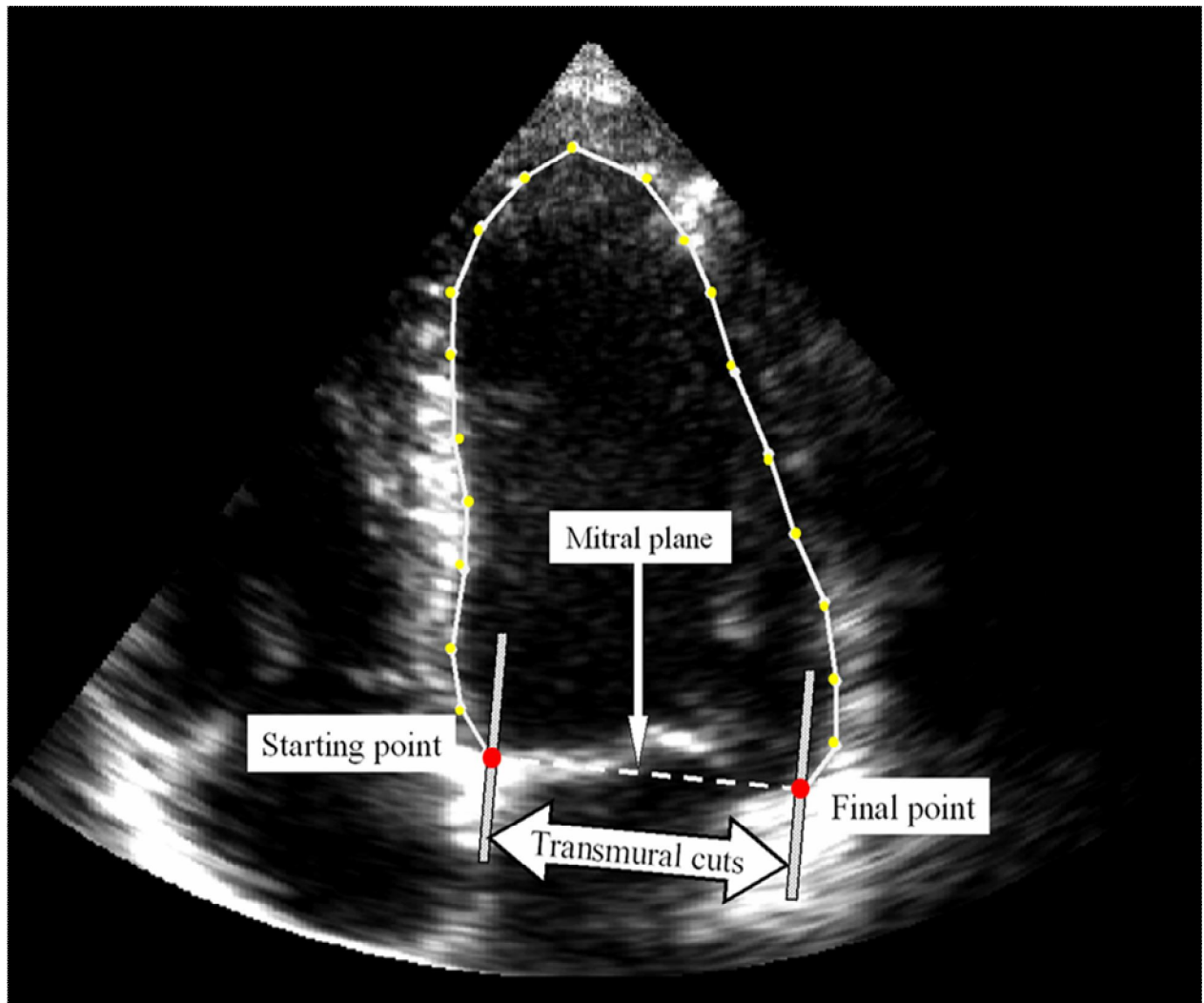
Fig. 15. A step in establishing the border tracking is recognition of the annular plane. 2 chamber view of the adult heart. Yellow markers are the points delineating the LV border, red points set by the operator act as anchors and help recognition of annular level due to spatial coherence. Figure adapted from (72).
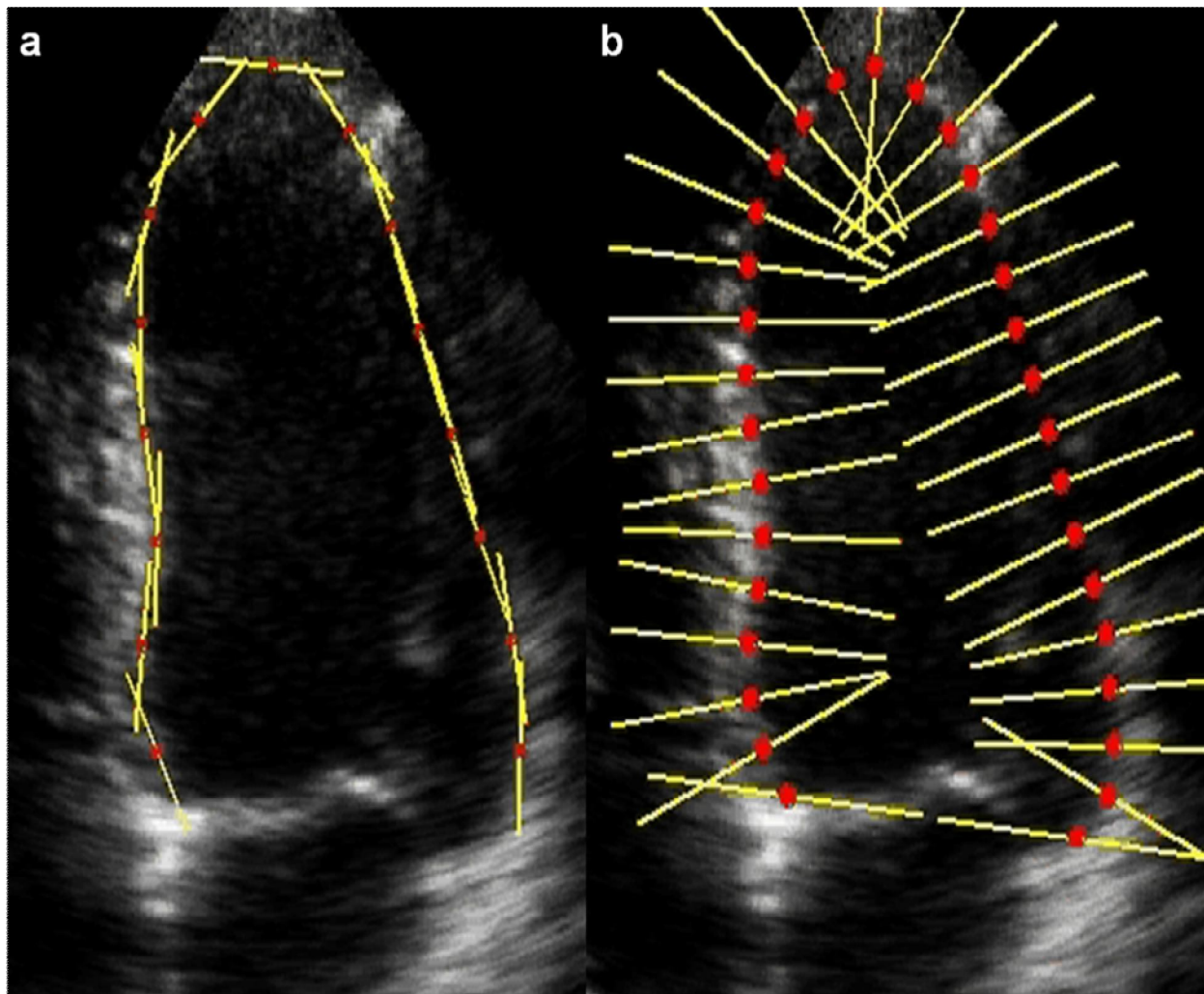
Fig. 16. An adult LV in end-diastole. (a) Imaginary bars indicate tracking along the longitudinal motion of the heart. (b) So-called „transmural cuts" represent tracking perpendicular to the long axis motion. Analysis in both directions occurs simultaneously. Figure from (72).
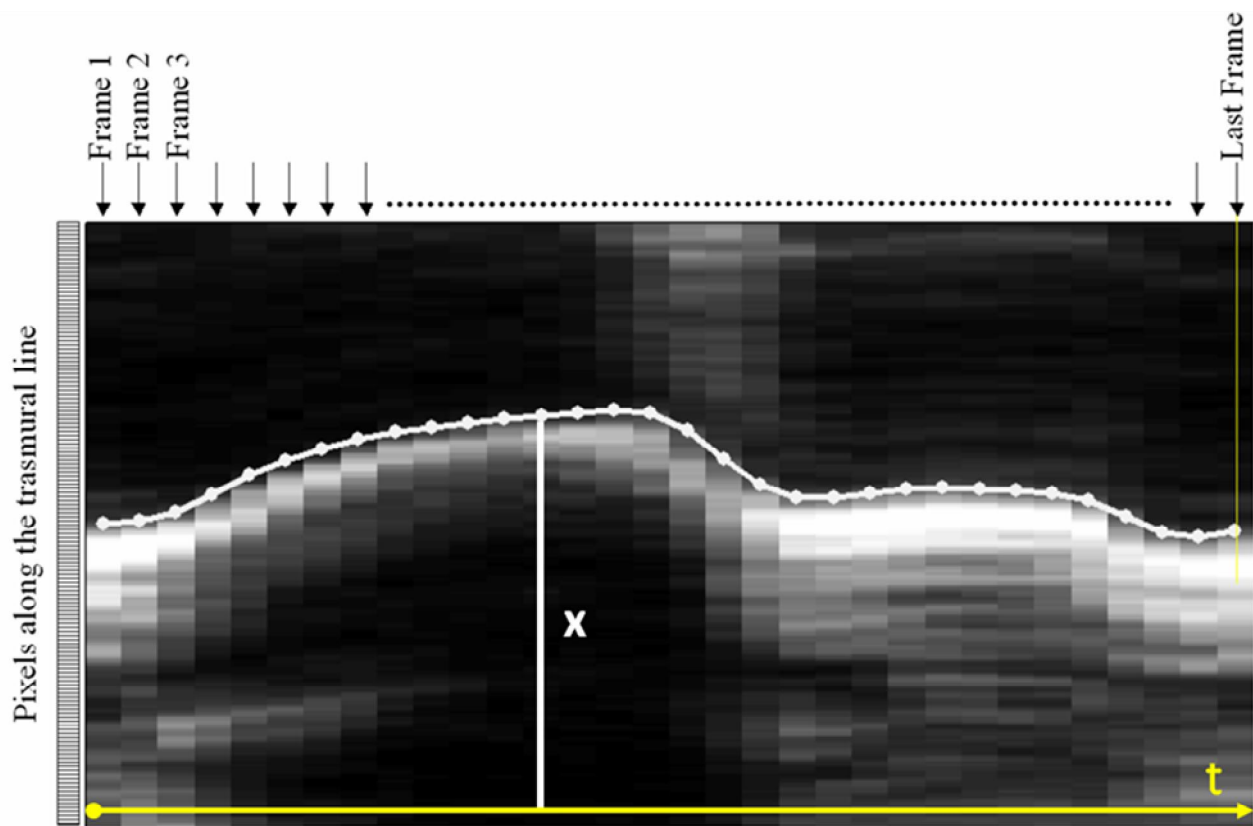
Fig. 17. This image shows how the transmural tracking and calculation take place. The pixels taken along one arbitrary transmural line from Fig. (16b) are placed in columns, each column corresponding to one frame of the sequence of images. In this way the evolution along a transmural cut can be represented in a two-dimensional representation where one axis is the distance (x) along the line and the other axis is the time (t). In this one-dimensional tracking the displacement between successive frames is estimated by evaluating the cross correlation between the actual and previous time instance (frame). To improve the reproducibility in the case of poor images with a low signal to noise ratio, the space time representation is built using a line for the transmural cut with a thickness larger than that of a single pixel and extracting the average value across such a thickness. In this application a 5 pixel thickness is employed. Annotation and Figure adapted from (72).

2.2.1.2. Tracking of Remaining Points

After the reference points have been tracked, the tracking of all the other points along the original border is performed with a two-dimensional technique. A square window of 16 pixels on each side of the current position of the point is extracted from all B-mode frames, then the frame by frame displacement in the horizontal and vertical directions that minimized the total brightness pattern convention error is computed by the least squares method that represents a 2x2 linear system that is solved analytically. This is performed in two steps with predictor-corrector strategy to improve the reliability of results (Figure 18).
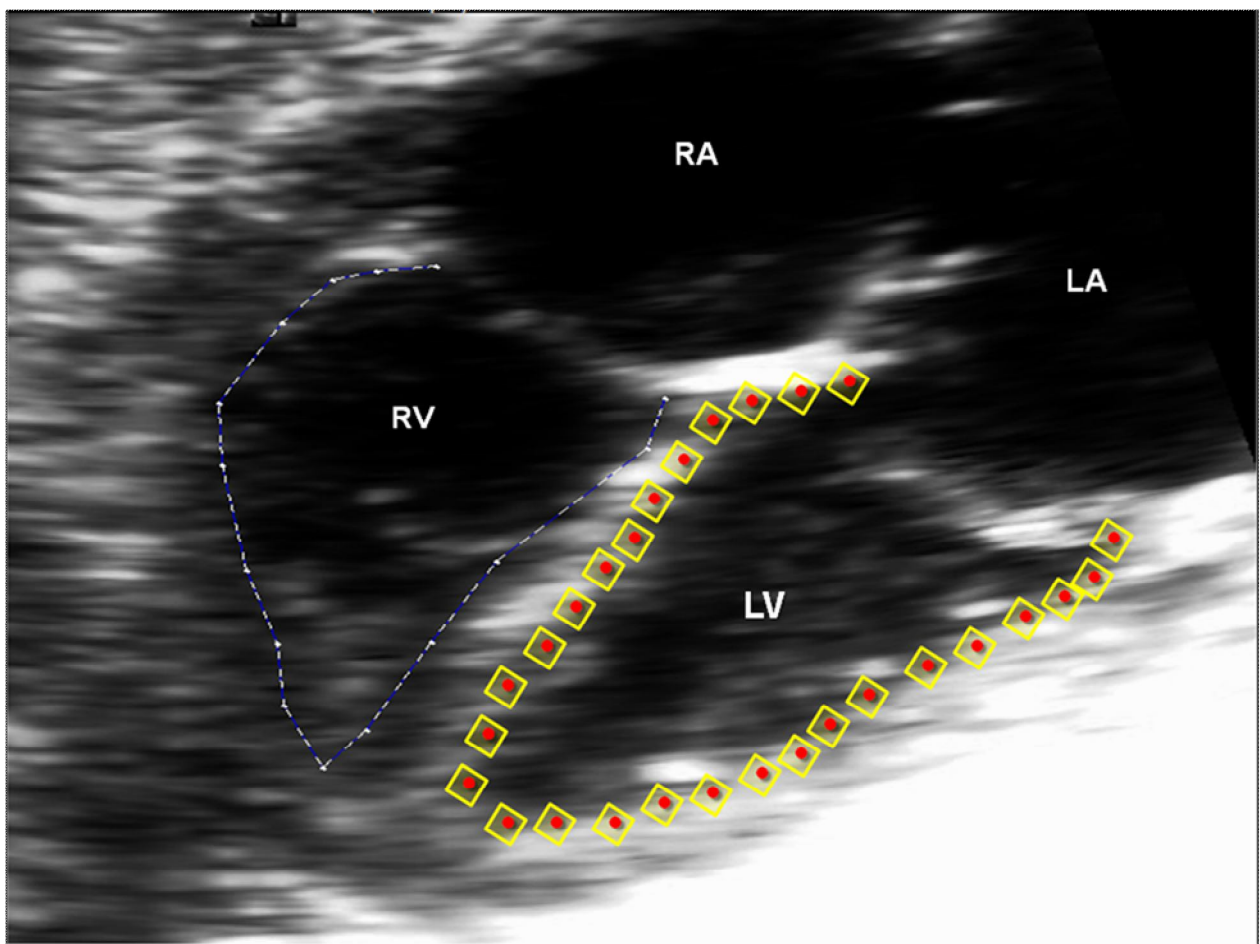

Fig. 18. A fetal heart at 33+2 week. RV is traced by the operator and ready to be processed. The more prominent white dots (along the RV border) are the reference points set by operator. Other points are put automatically as a result of tracing. The searching algorithm for non-reference points utilizes a 4 pixel by 4 pixel square tracking approach in every frame. To not superimpose the actual trace and the illustration of searching algorithm, the square method is shown at LV.

2.2.1.3. Application of a Sequence of Intermediate Passages. Fourier Transformation using the Periodicity of the Heart Motion.

For each point, independently, a further sequence of one-dimensional tracking along specified directions is performed by using again the method of transmural cuts. A line crossing the wall, passing through the point, and directed normally to the current border is drawn, this operation is made for each frame because the points are not fixed in time but they have been displaced at each instant accordingly to the previous tracking steps. At this stage all the original points have been tracked in time, each one independently, and over all frames. In all tracking steps, a spatial coherence in the tracked border is ensured by applying a 3 point median filter and a 3 point Gaussian filter (of weights 0.25, 0.5, 0.25) for the displacement computed at neighboring points.

2.2.1.4. Border Strain, Strain Rate and Displacement

The one-dimensional strain and strain rate are evaluated along the border. In the present application the strain rate is computed from the velocity by the general formula

$$\frac{1}{L(t)}\frac{dL}{dt} = \frac{dV_s}{ds} + \frac{V_n}{R};$$

L: lenght
t: time
V: velocity

where the subscripts s and n indicate the velocity vector components along and vertical to the border, respectively; R is the local radius of the curvature. The geometrical interpretation of this formula is shown in Figure 19.
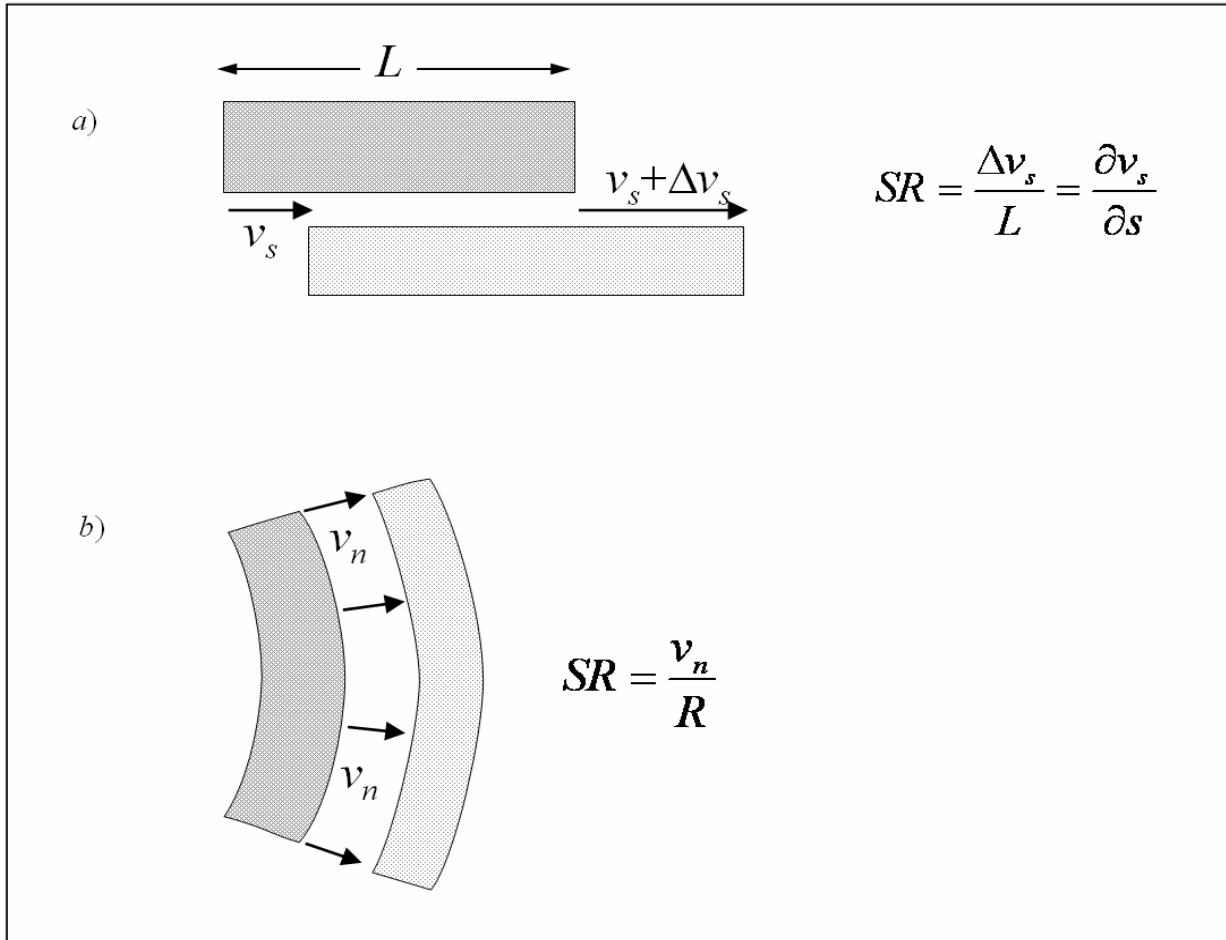
Fig. 19. The strain rate is given by a differential longitudinal velocity along the tissue (*a*), or by a velocity vertical to a curved segment (*b*). This offers a more correct strain computation along curved myocardial segments Figure from (72)

This formula is an exact expression for the case of a generic plane curve subjected to a two-dimensional velocity. The strain is then computed by integration from the strain rate as by the definition;

$$SR(t) = (St + 1)^{-1} \frac{dSt}{dt}, \quad St(t) = \exp \int_{t_0}^{t} SR(t') dt' - 1.$$

These estimations take into account the knowledge of the two-dimensional velocity vector, and the curvature of the tissue. Therefore, the result includes contributions that are not apparent using the TDI approach (70, 73). Furthermore, this approach allows the analysis of apical regions that cannot be properly processed with TDI data. The estimation of local frame-to-frame displacement accompanies the assessment of the

local velocity since velocity is the ratio between displacement and time interval. Calculation of the displacement therefore is determined by local velocity differences multiplicated by time period between consequent frames. A summarizing calculation cascade is shown in Figure 20.
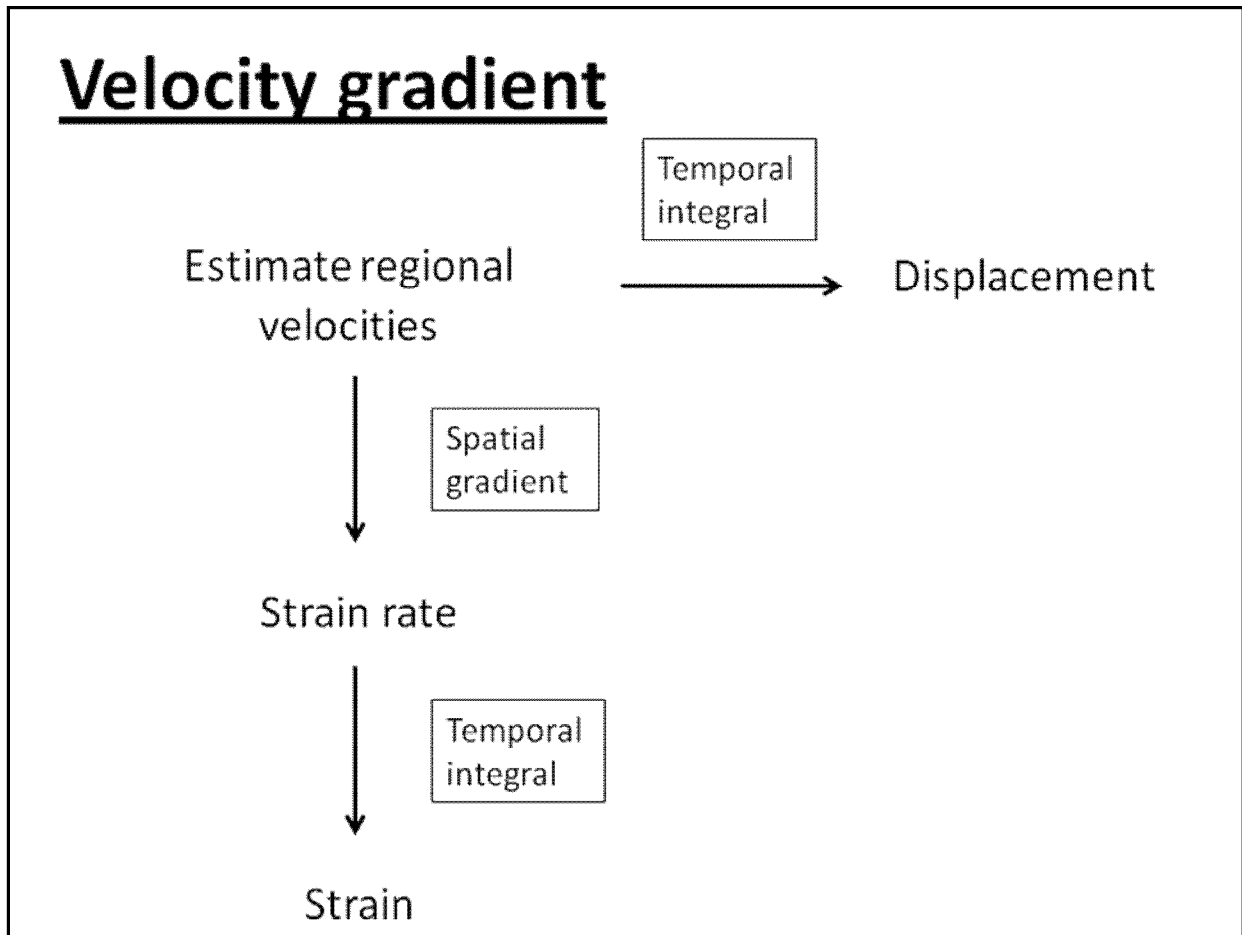

Fig. 20. Schematic overview of the operations required for strain, strain rate and displacement estimation in the velocity gradient methodology used in VVI.

2.3. Study Collective

2.3.1. Recruitment of Participants, Inclusion / Exclusion Criteria

We asked in the time period from 28.02.2009 to 07.08.2009 pregnant women who came to First- and Second-Trimester Screening and routine follow-up examinations to the Department of Obstetrics at Campus Virchow Klinikum to participate in our study. Additionally we recruited in-patients who were admitted via the delivery unit. We explained the need for echocardiographic four chamber (4Ch) view for research purposes and gave an information leaflet which outlines our aims and evaluation method. Informed consent has been taken from the participants.

- Only singleton pregnancies have been included in our study.

- Major cardiac anomalies were an exclusion criterion.

- Independent of the smoking status and systemic diseases of the mother and estimated fetal weight all singleton pregnancies were included in the scanning according to our study aim No.1.

- According to study aim No.2. data from pregnant women with systemic diseases like Type I/II Diabetes Mellitus, Gestational Diabetes Mellitus, HIV, maternal hypertension, etc., data from smokers or persons who were in our drug substitution program and data from fetuses whose weight was not appropriate for their gestational age have been excluded and have not been taken into consideration.

Two hundred thirty women agreed to participate in the study. Examination data of ninety-three pregnancies could not be analyzed and excluded due to several factors like experience level of the examiner, time limit set for the examination (10 minutes), excessive fetal movement, poor image quality, unfavorable fetal lie, no possible tracking of fetal heart ventricles despite adequate image quality and technical problems. One hundred thirty-seven echocardiographic examination data included in the feasibility evaluation with Feature Tracking Algorithm. In sixteen cases the ventricles needed to be assessed in different digital loops due to inaccurate tracking results despite adequate imaging or poor lateral resolution. In 40 cases it was not possible to evaluate both ventricles in the same image. Table 1 summarizes the feasibility of VVI.

Table 1. Feasibility of Image Evaluation	Number of Cases
Both ventricles evaluated in single digital loop	81
Both ventricles evaluated in seperate digital loops	16
Only LV could be evaluated	23
Only RV could be evaluated	17
Excluded from the study	93
Total	**230**

From one hundred thirty-seven cases sixty-two right ventricular and sixty-eight left ventricular assessment were included into final analysis.

2.3.2. Maternal Characteristics

Age:

- Range was 18-45 years of age. Median age was 31 and mean age was 30,4.

Preexisting Conditions of Study Participants:

- 22 % of mothers were smokers.

- Approximately 5 % of women has HIV.

- 10 % was diagnosed with Type I/II or Gestational Diabetes Mellitus (GDM).

2.3.3. Fetal Characterictics

Gestational Age:

- Range of gestational age was $13^{+0} - 41^{+3}$ week. Median gestational age was 31^{+4} and mean gestational age was 30^{+2} week.

Discrepancies in Estimated Fetal Weight:

- 4 fetuses have been diagnosed with Intrauterine Growth Restriction (IUGR). Mothers of three IUGR fetuses were smokers. 4 fetuses had been diagnosed with being Small for Gestational Age (SGA). One fetus was large for his gestational age who belonged to a mother diagnosed with GDM. All other fetuses were appropriate for their gestational ages.

Fetal Echocardiographic Examination:

- All fetuses included in the study were examined echocardiographically either by a physician in a private office or by one of our senior physicians (Prof. Dr. W. Henrich and Dr. M. Brauer) in the Department of Obstetrics at Campus Virchow Klinikum who have specialized in obstetric and gynecologic ultrasound and have many years of experience with fetal echocardiography. All fetuses had unremarkable echocardiographic examinations and no rhythm disturbances except one who had 2 small muscular ventricular septal defects with unremarkable amniocentesis result.

2.4. Evaluation Method

2.4.1. Ultrasound System and Transducers

For this study we worked with Acuson S 2000 (Siemens Medical Solutions USA, Inc., Mountain View, CA, USA). The ultrasound system has three transabdominal transducers; one linear (9L4, frequency range in 2D-Mode: 4 MHz - 9 MHz), one curved (6C2, frequency range: 2,5 MHz – 6 MHz) and one 3D transducer (7CF2, frequency range: 3 MHz – 6,5 MHz). The endocavity transducer has not been used in this study.

Picture 1. Siemens Acuson S 2000 ultrasound machine in an examination room in the Klinik für Geburtsmedizin at Campus Virchow Clinic. This ultrasound system was able to take video clips in relatively high frame rates without compressing the image information.

2.4.2. Scan Settings

For image acquisition we implemented the following scan settings to reach frame rates as high as possible in order to prevent possible underestimation of values assessed with Feature Tracking Algorithm;

- SieClear - Advanced SieClear: This multi-view spatial compounding feature, used to reduce speckle formation and enhance tissue differentiation in 2D-mode images, has been disabled to foreground speckles and improve the frame rate.

- Space-Time: This option adjusts the balance between the image line density (resolution) and the frame rate. Increasing the line density increases resolution and decreases frame rate. It has four levels. We disabled this option fully to acquire images with high frame rates.

- Tissue Harmonic Imaging (THI): We enabled THI to enhance contrast resolution.

- Persistence: Persistence creates a visible smoothing effect by maintaining lines of image data for each frame of imaging. A higher setting includes more frames in the image data. It has four levels (from 1 to 4). We chose the "level 2" since this proved to be more suitable for Tissue Tracking analysis.

- Dynamic Range (Dyn R) and Frequency: To enhance the overall contrast resolution we adjusted Dyn R, and depending on the depth of the fetal heart and maternal abdominal constitution we set the adequate frequency.

- Edge Enhancement: This feature distinguishes the contours of a structure during imaging. It has three levels (from 1 to 3). We selected the "level 2" for our imaging.

- Zoom – Depth – Focus: For the purpose of the study special attention was paid to get a highly zoomed-in digital image. The imaging depth and focal zone marker were adjusted for an optimal image.

Picture 2. The console of the ultrasound system and presets recommended by the provider to capture video clips for evaluation with Velocity Vector Imaging (VVI) software. VVI is the trade name of feature tracking algorithm registered by Siemens Medical Solutions, USA.

2.4.3. Data Acquisition

After displaying the abdominal circumference care has been taken to visualize the fetal heart in 4Ch view without any reverbaration artifacts and shadowing from fetal parts, paying attention to demonstrate the apical region of the cardiac chambers. When the fetus was quiet at least two consecutive heart cycles were observed. In the presence of breathing excursion of maternal abdomen the mother kindly requested to hold her breath for a couple of seconds. Following the observation of several fetal heart beats the real-time imaging was freezed, with the help of the control wheel the ideal digital loop sequence was sought retrospectively and recorded utilizing "Acoustic Clip Capture", a feature which acquires digital video clips with a time interval between two frames less than 34 milliseconds (msec). A simultaneous video clip capturing during the actual examination was not possible. This approach has been repeated until sufficient amount of digital loops were gathered respecting the 10 minutes time limit for examination. At the end of the recordings the serially numbered and anonymized patient data were saved on digital versatile discs.

Our recordings for LV have an average frame rate (FR) of 114 frame per second (fps); range 57-241, median 104, and for RV an average FR of 113 fps; range 52-241, median 103. The time between two frames (TBTF) was for LV 10 milliseconds (ms) in average with a range of 5-33 ms, median 10 ms. For RV we had a TBTF of 11 ms in average with a range 5-33 ms and median was 10 ms.

2.4.4. Software and Hardware

The acquired digital loops in 4Ch view were evaluated offline with syngo Velocity Vector Imaging (VVI) software package (Siemens Medical Solutions USA, Inc., Mountain View, CA, USA) on a Packard Bell computer (2,5 GHz, 4 GB Ram).

2.4.5. Data Processing with syngo VVI

Firstly, obtained data are uploaded to the internal memory of the software. Then for each case the clip with the best endocardial border definition was chosen to begin with the processing. The processing of a raw data starts with setting of virtual R-Waves to define cardiac cycles. Although the visual confirmation of opening (start of the diastole) and closure (start of systole) of atrioventricular (AV) valves helps determining a cardiac cycle, we utilized the "Anatomical M-Mode" function incorporated into the software to guide our placing the R waves as seen on Figure 21.

After defining at least two cardiac cycles we move on to the next step in which we establish a trace along the endocardial border. The definition of the endocardial surface takes place by putting several points along the endocardium mostly at the end-diastole (when the endocardial border is better visible) as seen on Figure 22.

Hereafter we let the algorithm process the trace and calculate the values which we collected for this study as performance parameters of fetal ventricular myocardium in its longitudinal axis. In regions with poor tracking (assessed subjectively), endocardial border was readjusted manually by resetting the point(s) along the endocardium until better tracking was achieved. Border definition by the user and border establishment are shown on Figure 23.
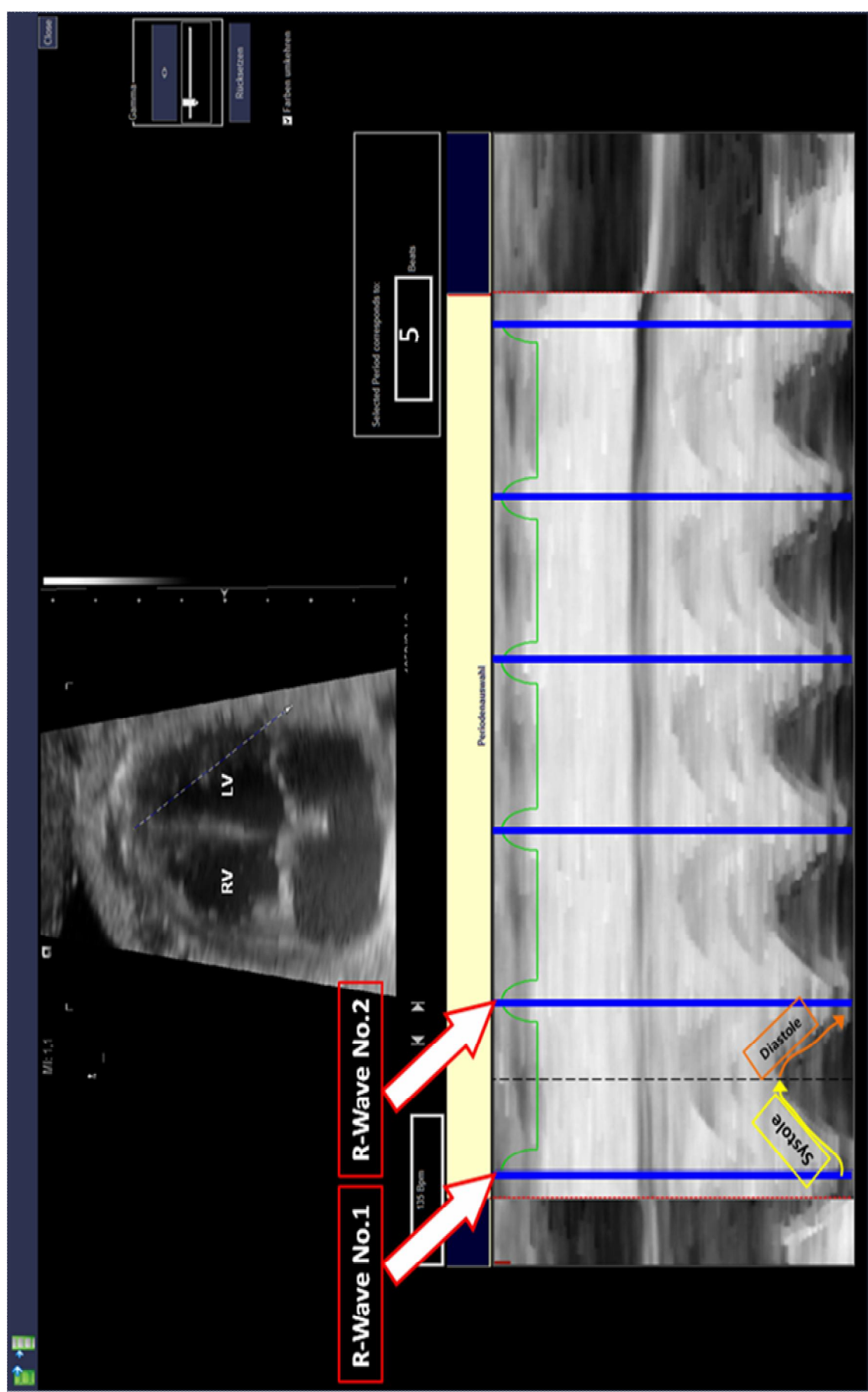
Fig. 21. Fetal 4 Ch-view at 26^{+1} week. M-mode cursor positioned at the left atrioventricular junction to record long axis motion after Gardiner et al. (65). Blue bars indicate R waves defining the beginning and end of a cardiac cycle.
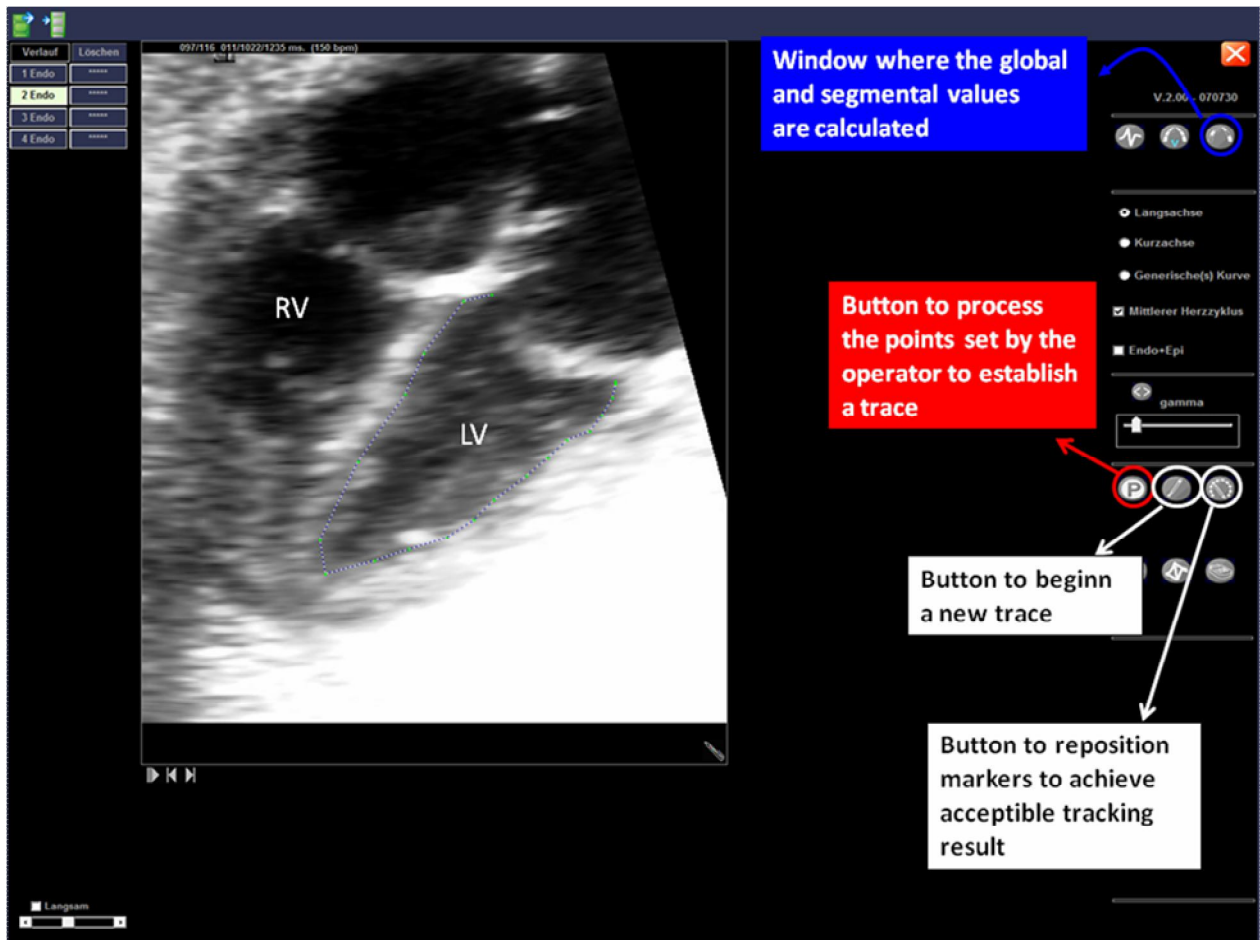
Fig. 22. Fetal LV at 33+2 week. This is the first window after defining the cardiac cycles. Screenshot has been modified due to place issue. This figure represents by the example of a LV the initial step of endocardial border establishment. Green points are the reference points placed by the user. Notice several other points smaller in size automatically placed by the algorithm.
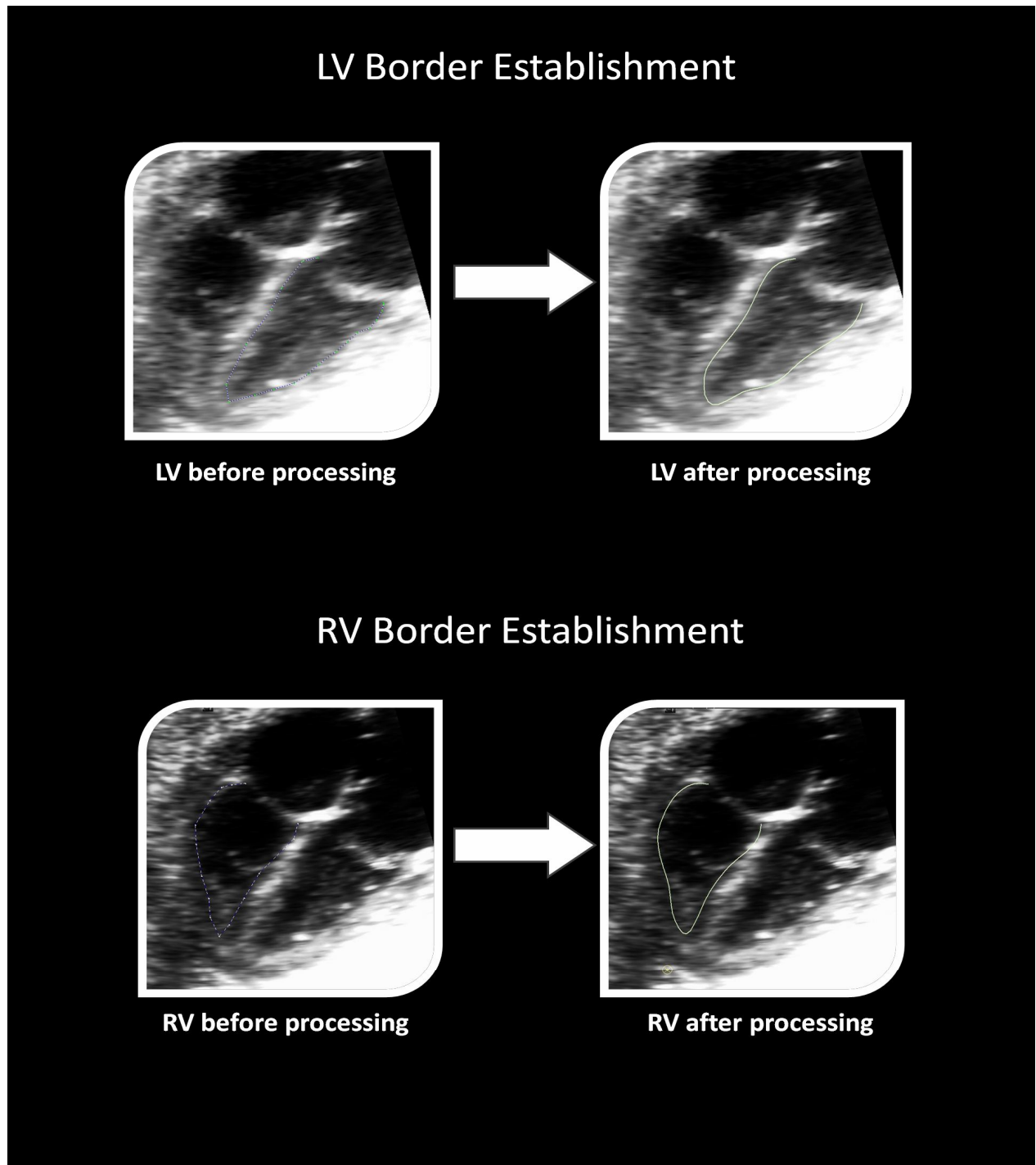
Fig. 23. After defining the endocardial border manually (left 4 Ch-views) we let the algorithm process and obtain a continuous line (right 4 Ch-views) which starts and ends at the AV valve level as shown in this figure.

2.4.6. Data Collection and Six-Segment Model to Assess Global Myocardial Function

According to the aims of this study we used the six-segment model to assess global myocardial function as depicted on Figure 24.
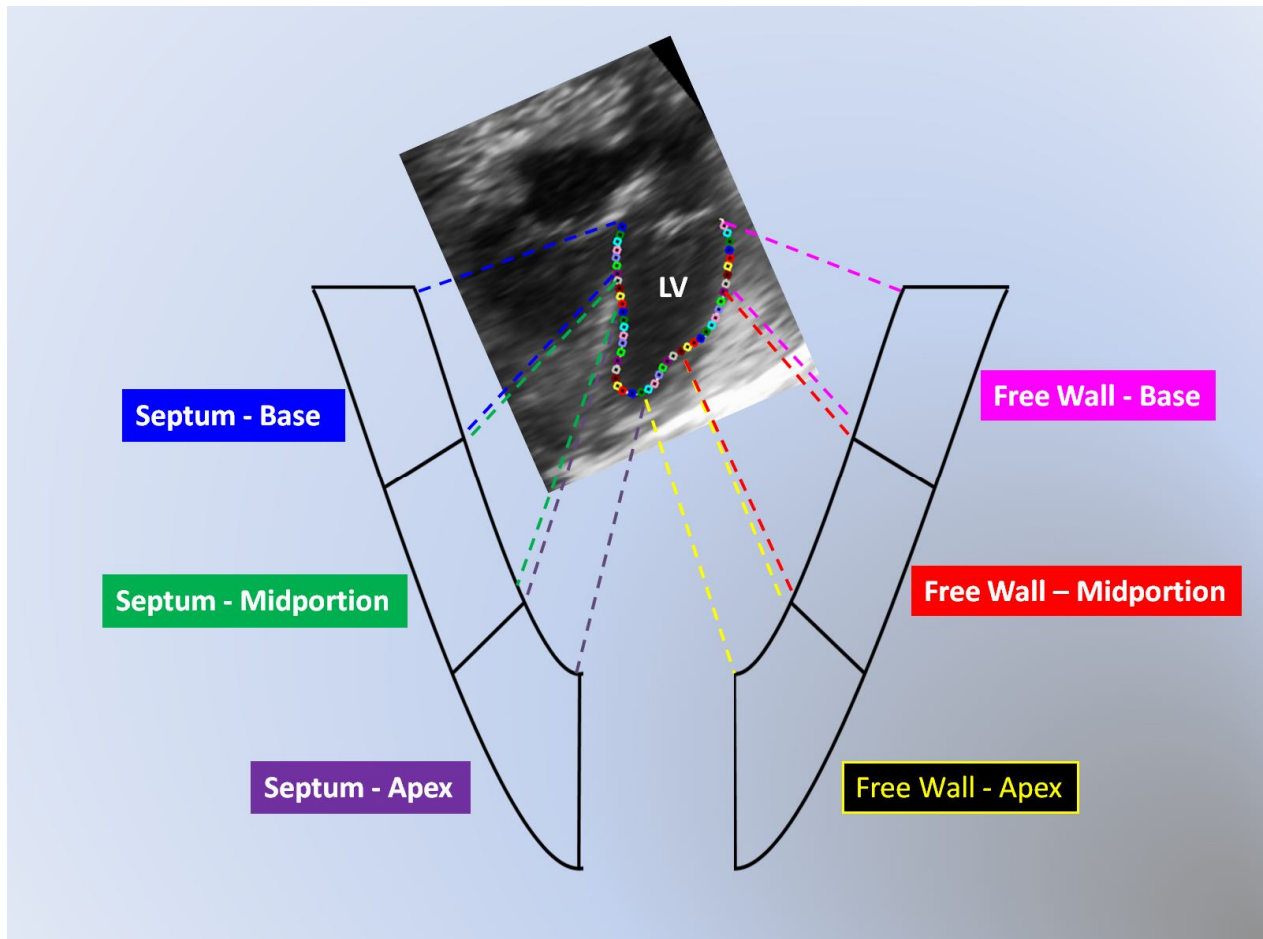
Fig. 24. The endocardial border of any ventricle is divided into 6 equi-distant lines. Every compartment has its own subregions which are represented by small colored rings. Any global value is the average of the sum of these 6 compartments.

In this model the endocardial border is shown in six equal-sized segments. Every segment consists of multiple small subregions and the tabularly displayed data are the average of these subregions in every segment (Figure 25).
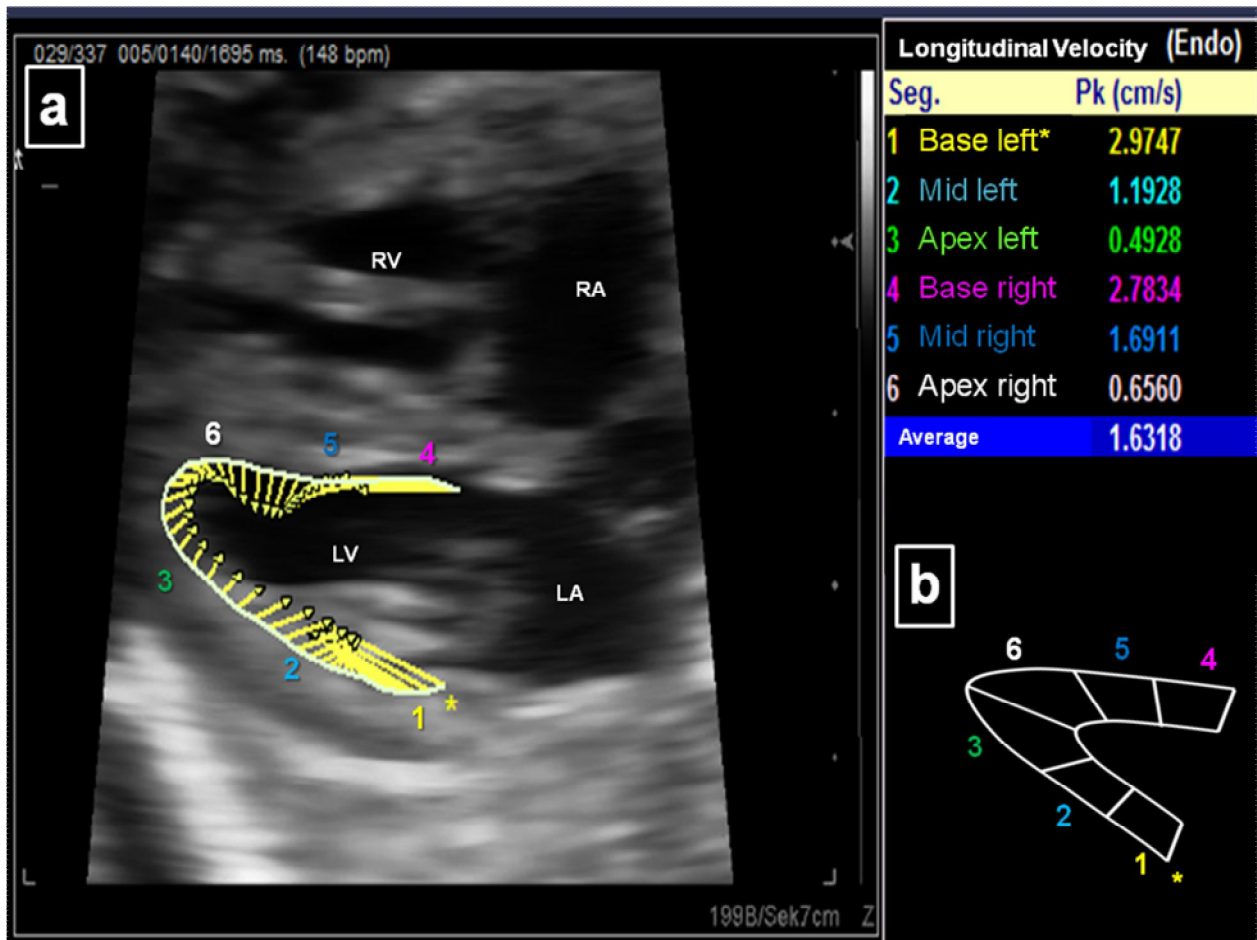
Fig. 25. Data collection by the example of velocity data. (a) Lateral 4 Ch-view. Processed LV endocardial border with its velocity vectors is seen. Numbers from 1 to 6 are to find in (b). The table shows the corresponding values for every segment and provides the average value at the end. The 6 segment model (lower right) is also shown to demonstrate the match between endocardial line and its segmentation.

We read the peak value for every parameter [Global longitudinal peak systolic and diastolic velocities (PSV and PDV), longitudinal peak systolic and diastolic strain rate (PSSR and PDSR), longitudinal peak systolic strain (PSS) and longitudinal peak displacement (PD)] from the table generated by the software (Figure 25) and exported the data into an Excel spreadsheet. We observed the form of every curve in systole and in diastole to assess whether the behavior of the curve corresponds with M-Mode recording. Despite using acoustic clip capture when saving digital loops the separation of diastolic velocities and strain rates into early and late phases could not be observed in most instances. We therefore reported one single peak value for diastolic velocity and strain rate. For a better comprehension we display representative graphs for all parameters evaluated (Figures 26-32).
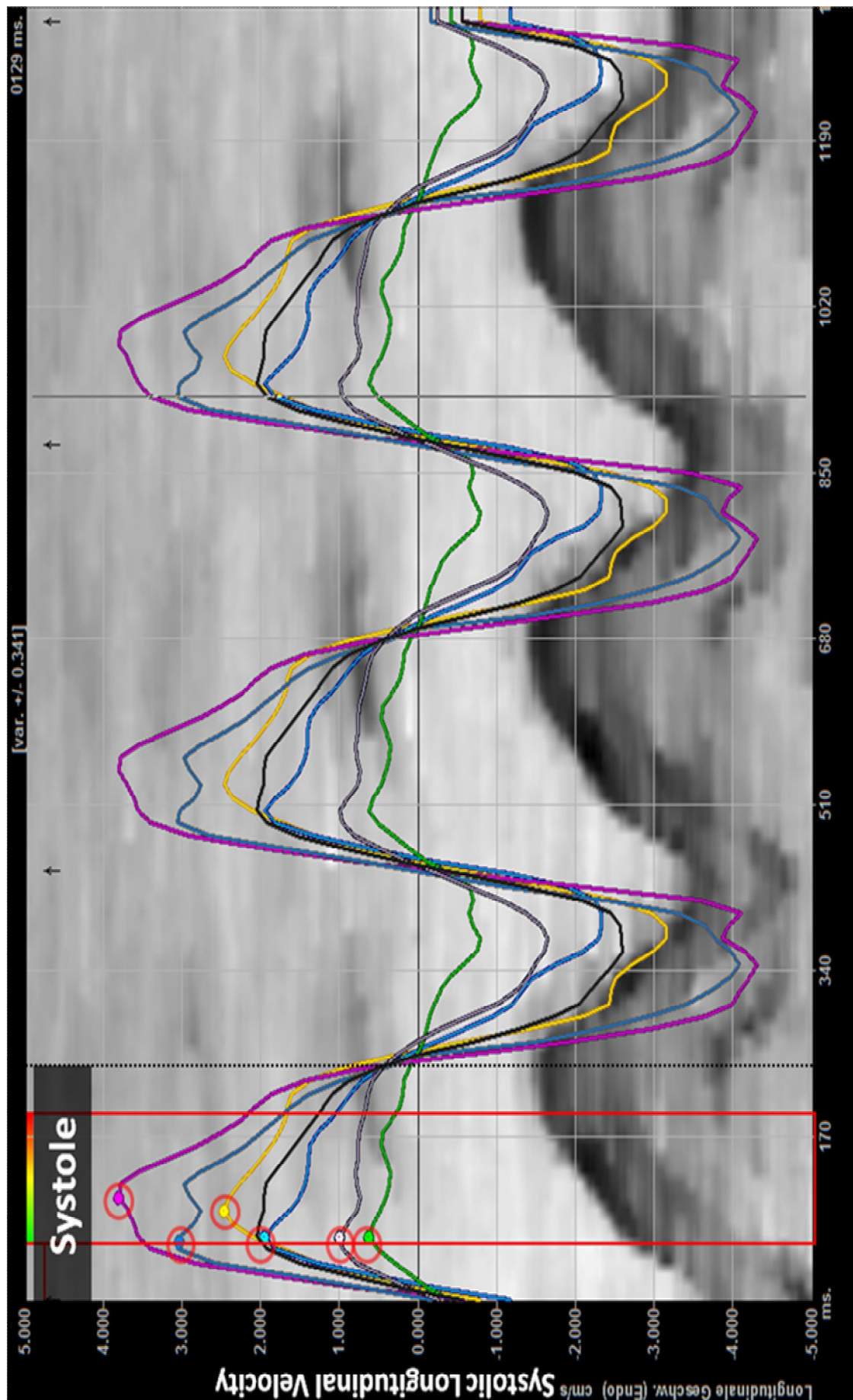
Fig. 26. Systolic velocities. Peak systolic velocities are indicated by red rings. Black dotted line seperates systole from diastole. A 7th black curve represents the average. Red bars can be adjusted freely by the user. This is a feature to support dyssynchrony analysis in adult cardiology and has not a particular function in our study. They can be positioned in a way to present systolic and diastolic values as seen in the next figure.
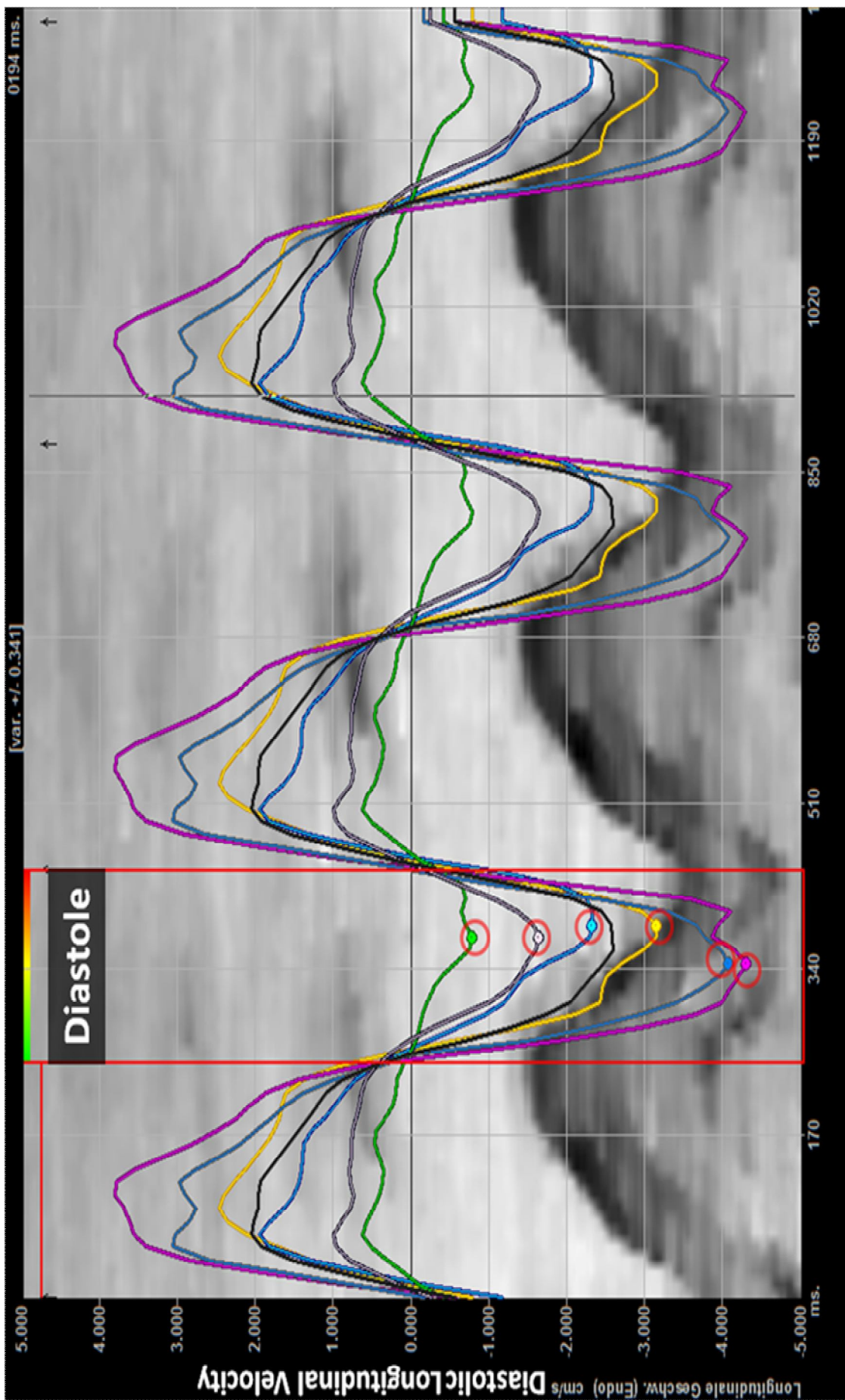
Fig. 27. Diastolic velocities. Peak diastolic velocities are indicated by red rings. Two red bars define diastole. A 7th black curve represents the average behavior of all segments (global performance)
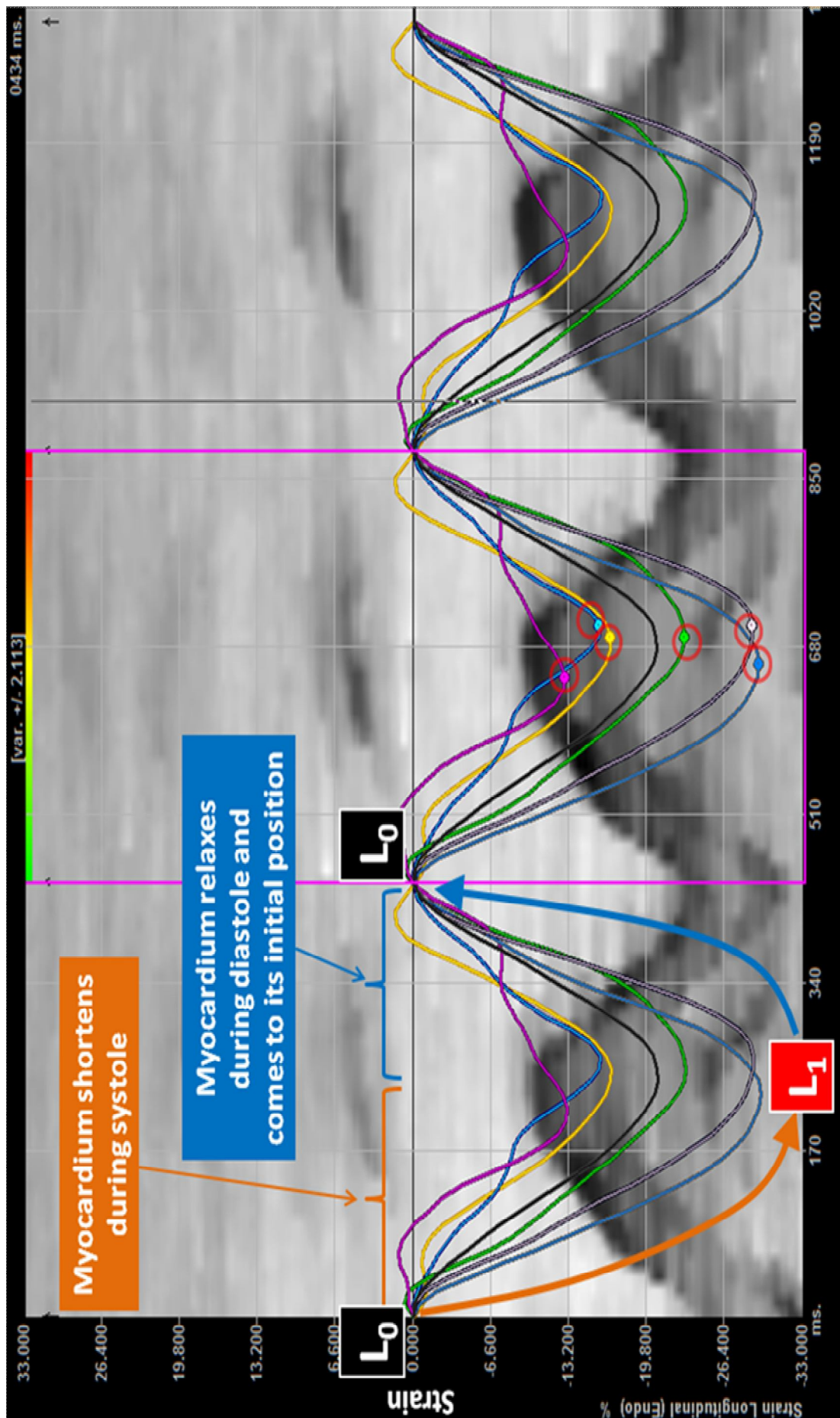
Fig. 28. Characteristics of Strain curve. Although the lowest value of strain constitutes a nadir, in the TTE literature it is established to use the term "Peak Systolic Strain" (PSS) to define the most minimum value a curve can get. PSSs are indicated by red rings. Two purple bars define a single cardiac cycle. Orange and blue colored curved arrows represent the typical course of strain during heart cycle
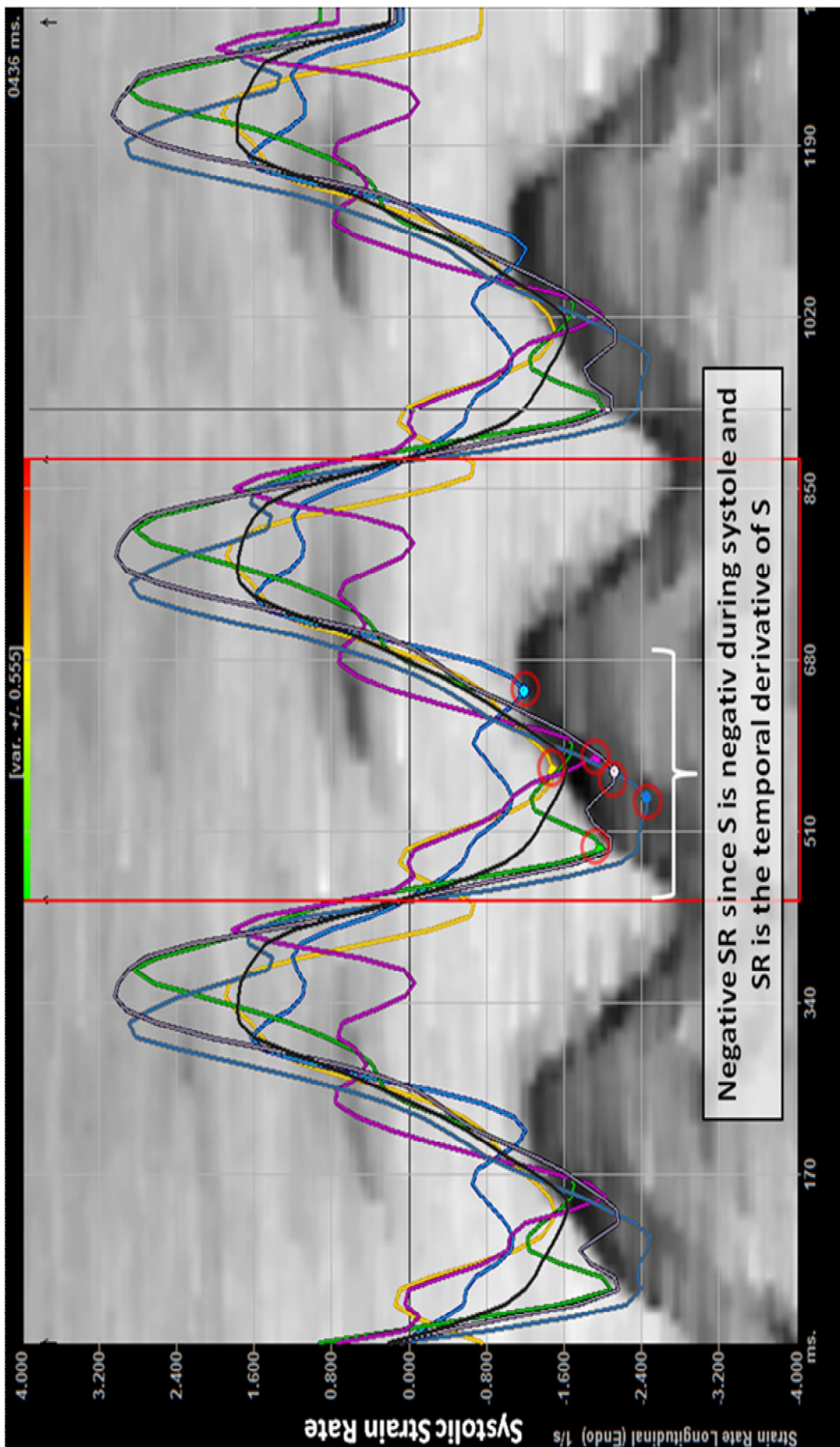
Fig. 29. Characteristics of Strain Rate curves. A typical SR curve has a biphasic behavior. Here the values during systole are shown. Peak values are indicated by red rings. Red bars define a single cardiac cycle. A 7th black curve represents the average behavior of all segments (global performance).
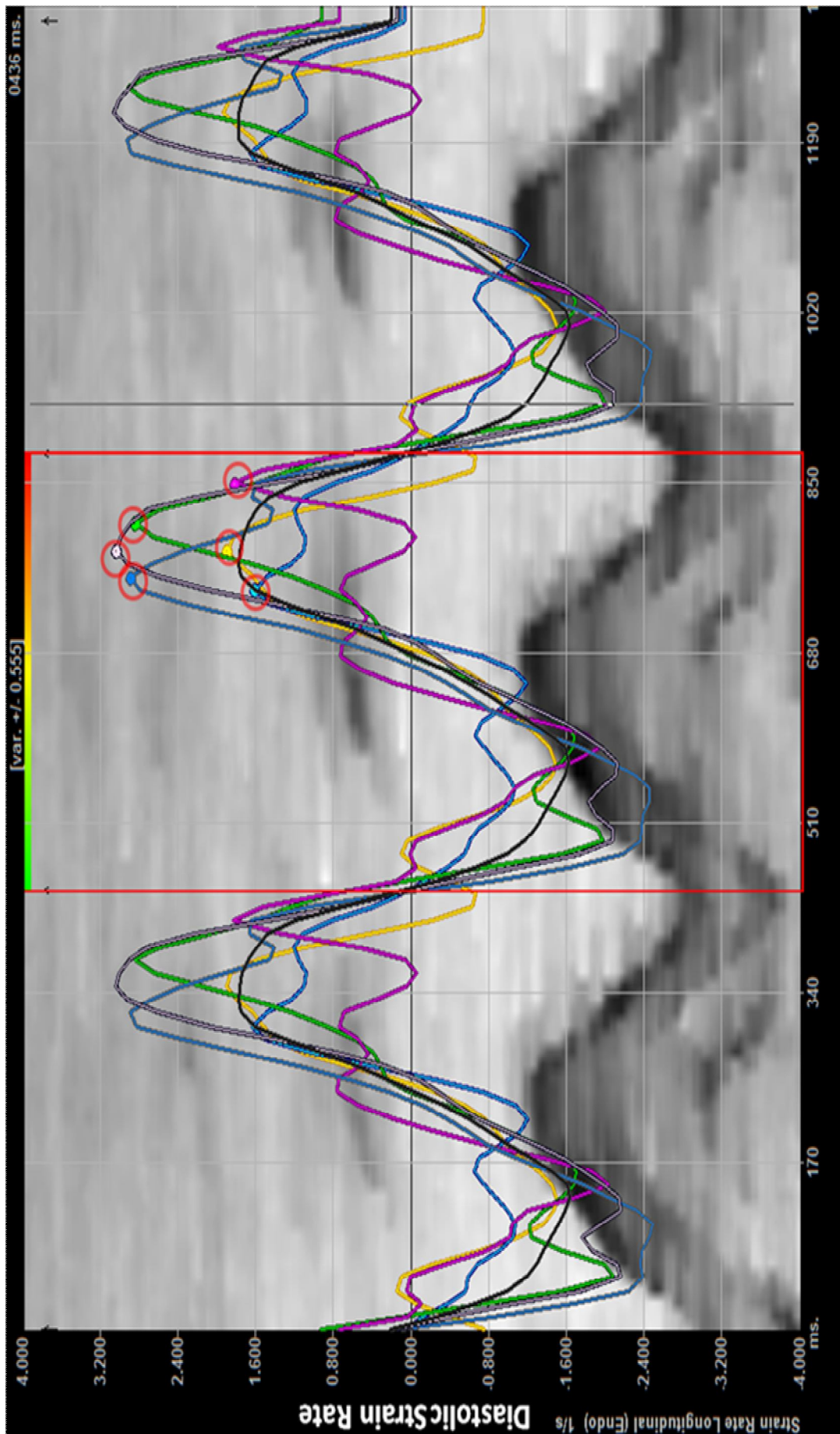
Fig. 30. Diastolic Strain Rates. Peak diastolic SRs are indicated by red rings. Red bars define on single cardiac cycle. A 7th black curve represents the average behavior of all segments (global performance)
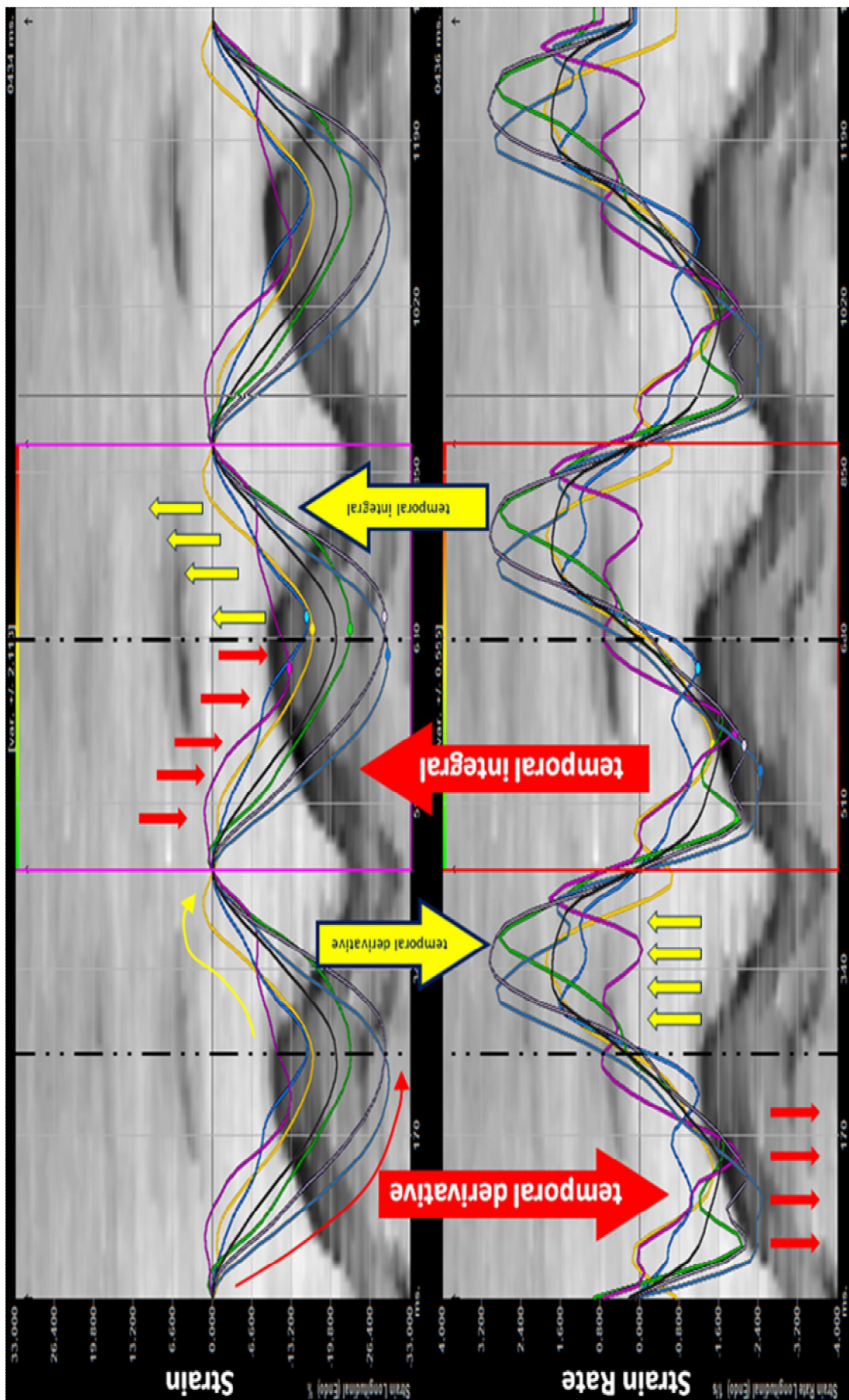
Fig. 31. Superimposed Strain and Strain Curves to emphasize the relationship between S and SR. Black imaginary lines drawn to help the reader distinguish the tendency of the curves readily.
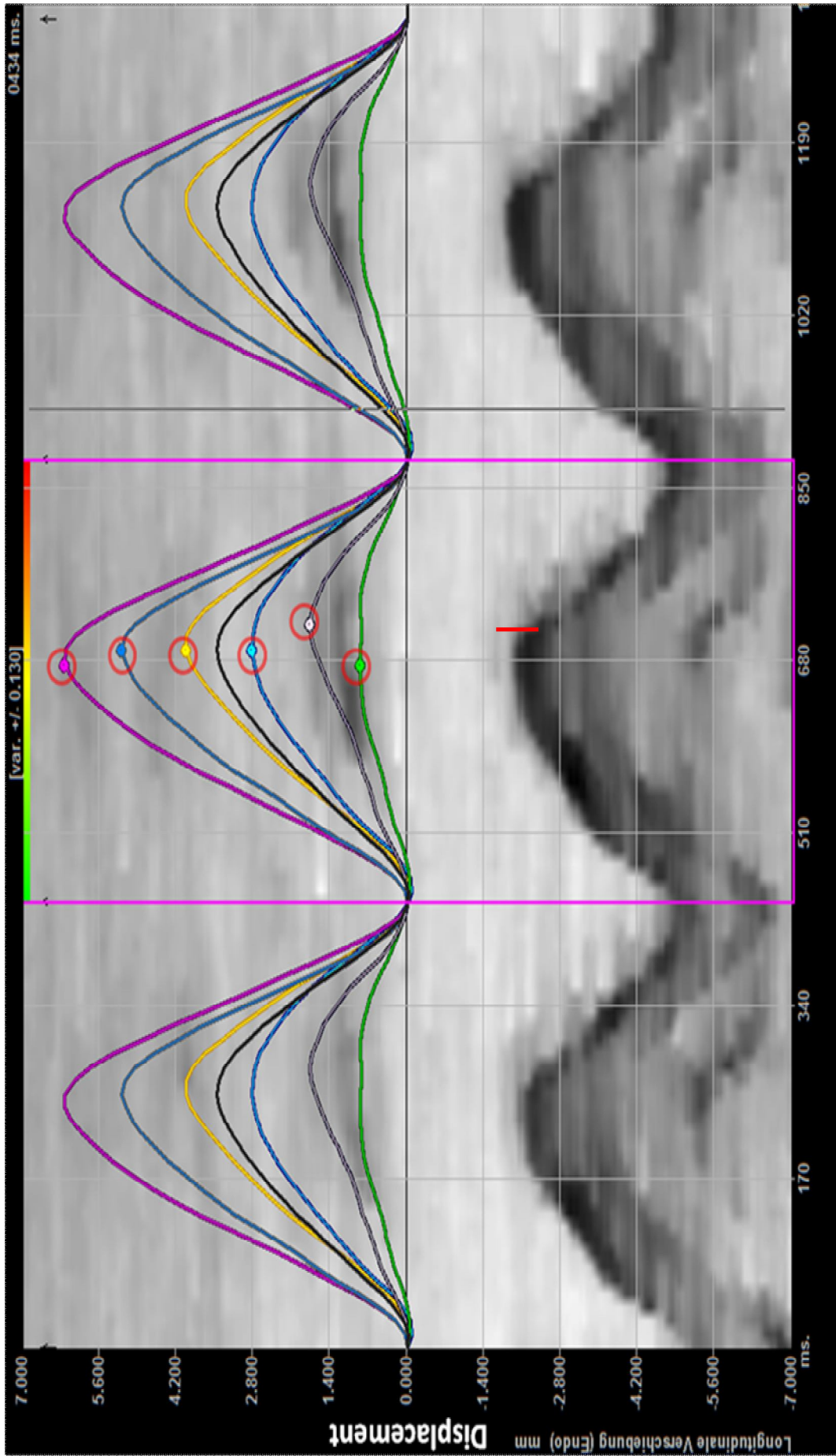
Fig. 32. Maximum displacement curves. Notice the acceptable alignment of peak values (red rings) and the end of systole indicated by the red bar on the M mode.

2.5. Statistical Analysis

All the data were expressed as mean ± Standard Deviation (SD) unless specified otherwise. Statistical analysis was performed using Statgraphics Centurion XV statistics package. Kolmogorov-Smirnov Test was used to assess the normal distribution of the data. Comparison of two groups has been done with Student-T-Test. Simple linear regression has been applied to do a regression analysis. Bland-Altman plots have been prepared in Microsoft Office Excel 2007.

2.6. Ethics Committee Approval

This study has been approved by the Ethics Committee of Charité Universitätsmedizin Berlin. (Prospektive, longitudinale Studie zur Erstellung von Referenzwerten der myokardialen Funktion des Feten durch Velocity Vector Imaging. Antragsnummer: EA2/025/09)